Quantum beats due to excitonic ground-state splitting in colloidal quantum dots

J. Bylsma, P. Dey, J. Paul, S. Hoogland, E. H. Sargent, J. M. Luther, M. C. Beard, and D. Karaiskaj

Phys. Rev. B **86**, 125322 — Published 26 September 2012

DOI: 10.1103/PhysRevB.86.125322

Quantum beats due to excitonic ground state splitting in colloidal quantum dots

J. Bylsma[1], P. Dey[1], J. Paul[1], S. Hoogland[2], E. H. Sargent[2], J. M. Luther[3], M. C. Beard[3], D. Karaiskaj[1*]
[1]*Department of physics, University of South Florida, 4202 East Fowler Ave., Tampa, Florida 33620*
[2]*Department of Electrical and Computer Engineering, Toronto, Ontario M5S3G4, Canada and*
[3]*National Renewable Energy Laboratory, 1617 Cole Boulevard, Golden, Colorado 80401, USA*

The dephasing of PbS quantum dots has been carefully measured using three pulse four-wave mixing and two-dimensional nonlinear optical spectroscopy. The temperature dependence of the homogeneous linewidth obtained from the two-dimensional spectra indicates significant scattering by acoustic phonons, whereas the excitation density dependence shows negligible excitation induced broadening in agreement with previous results. The rapid dephasing is attributed to elastic scattering by acoustic phonons. However, two dephasing components emerge, the short component that dominates the decay and a weaker longer decay, likely due to 'zero-phonon' dephasing. Quantum beats originating from two separate states can be observed, possibly revealing a $\sim$23.6 meV splitting of the excitonic ground state. Finally, the emergence of biexcitonic effects enhanced by the high quantum confinement is discussed.

PACS numbers: Valid PACS appear here

I. INTRODUCTION

The dephasing dynamics of electrons in semiconductor quantum dots have received recent attention because of quantum computing devices, whereas lead chalcogenide quantum dots have been the focus of recent studies largely due to the discovery and characterization of multiple exciton generation or carrier multiplication in these materials[1–3]. Models attempting to explain the process of carrier multiplication that have been proposed suffer from insufficient information about the structure of the excitonic ground state[4]. The dephasing dynamics exhibited in the coherent response of semiconductors is directly related to both, the electronic structure of the excitonic ground state and the many-body interactions taking place. The diffracted signal in a four-wave mixing (FWM) experiment measures explicitly the coherent response of the semiconductor. In three pulse FWM, three pulses are incident on the sample in directions $\mathbf{k_a}$, $\mathbf{k_b}$, and $\mathbf{k_c}$. The nonlinear interaction gives rise to a signal in the direction $-\mathbf{k_a}+\mathbf{k_b}+\mathbf{k_c}$. The phase conjugate pulse $-\mathbf{k_a}$ and the second pulse $\mathbf{k_b}$ are separated by the time delay τ whereas pulse $\mathbf{k_b}$ and third pulse $\mathbf{k_c}$ are separated by the population time T (Fig. 1 (b)). By varying the time delay τ and monitoring the FWM intensity, referred as time integrated FWM, the dephasing time of excitons can be measured. In order to monitor the third time evolution t additional time resolved experiments need to be performed. Measuring the dephasing time can provide a measure of the homogeneous broadening of the system. Recently, greater insight has been obtained by extending the methods of multidimensional Fourier-transform spectroscopy into the optical domain. In the present two-dimensional Fourier transform (2DFT) experiments the time delays τ and t are monitored simultaneously and the phase information is preserved. The Fourier transform with respect to these two time delays leads to a two-dimensional map in frequency domain where the ω_τ and ω_t axes are now correlated. It is the phase preservation throughout the experiment that makes these measurements challenging. In particular, in the optical frequency range minute mechanical drifts can lead to significant phase drifts comparable to the wavelength that would lead to inadequate 2DFT spectra. However, instrumentation developed recently consisting of an ultrastable platform of nested and folded Michelson interferometers that can be actively phase stabilized can overcome these challenges[5]. The advantages of multidimensional spectroscopy are well documented in the literature[6]. In semiconductor nanomaterials, 2DFT spectroscopy has allowed accurate measurements of the homogeneous linewidth and provided insight into the microscopic details of the many-body interactions[7–10].

II. RESULTS AND DISCUSSION

In this article we combine time integrated FWM measurements with excitation density and temperature dependent 2DFT spectroscopy to probe the dephasing mechanism and the electronic structure of excitons in PbS quantum dots. Time integrated FWM measurements at different T delay reveal an underlying long zero-phonon dephasing component besides the rapid decay due to exciton-acoustic phonon scattering. Quantum oscillations between two states split by the intervalley coupling with an energy separation of ~ 23.6 meV reveal a splitting of the excitonic ground state predicted theoretically[11]. High quality drop cast films of PbS quantum dots were prepared with the intent of minimizing scattered light. Absorption spectra of the films showed the usual 1s exciton peak centered at 833 nm, corresponding to ~ 3 nm diameter. The quantum dots were kept in vacuum and in thermal contact with the liquid helium cooled finger inside the cryostat. The FWM signal was collected in reflective geometry as shown in Fig. 1 (a) by mounting the cryostat at a small angle off-normal. The implementation of this geometry was very advantageous since it reduced significantly scattered light and distortions of the beams experienced in transmission measurements. The nonlinear response of semiconductors can in most cases be described by the third-order polarization induced by the optical fields. In semiconductors the Coulomb interaction between various polarization components cannot be ignored and the optical Bloch equations must be suitably modified to include Coulomb correlations. For an inhomogeneously broadened system, if the second pulse arrives after a time τ short compared to the dephasing time T_2, it reverses the phase evolution leading to the known photon echo. The colloidal PbS quantum dots are a strongly inhomogeneously broadened system due to their variation in size, therefore the time integrated FWM decays as $exp(-4\tau/T_2)$, where T_2 is the dephasing time and is related to homogenous linewidth according to $\gamma = 2\hbar/T_2$[12]. The time integrated FWM signal was collected at 5 Kelvin and the data is shown in Fig. 2 (a) together with single exponential fit and the instrumental response. The signal decayed as $exp(-4\tau/T_2)$ with $T_2 \sim 440fs$. From the measured dephasing time T_2 a homogeneous linewidth of ~ 3 meV can be obtained, in agreement with previous measurements[13]. Low energy acoustic phonons can efficiently scatter excitons in the highly degenerate spin states within the manifold in PbS quantum dots and are generally thought to be the mechanism behind the rapid dephasing in colloidal quantum dots[13–18].

However, 2DFT spectroscopy offers a more elegant and direct way of measuring the homogeneous broadening. While the profile along the diagonal of the 2DFT spectra marked with a dashed line in Fig. 3 (a-c) reflects the width of the inhomogeneous exciton ensemble excited, the cross diagonal profile provides a direct measure of the homogeneous

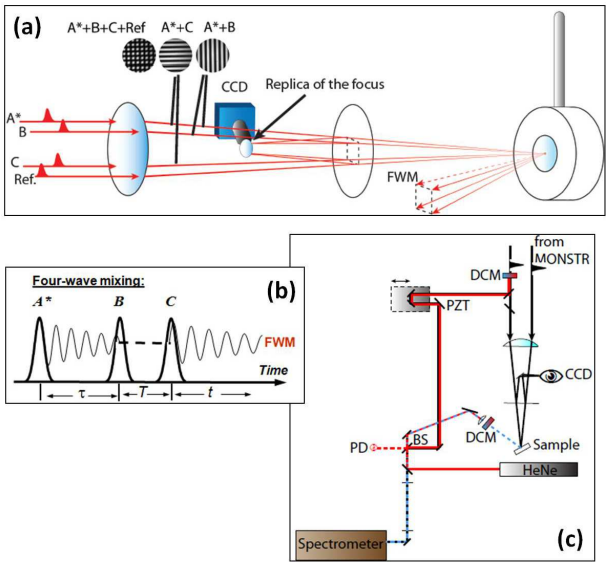

FIG. 1. (a) The four phase stabilized linearly polarized beams obtained from the MONSTR instrument described in Ref. 5 are focused on the sample, which is held in the cryostat at 5 K. The cryostat is mounted at a small angle with the perpendicular to the excitation beams in order to allow for the FWM signal to be collected in reflective geometry. A replica of the focus is monitored with the CCD camera. The interference pattern between the beams is used to obtain the phase difference between laser pulse pairs. (b) The sequence of the laser pulses used in the experiments, where A^* corresponds to the phase conjugate pulse. (c) Top view of the experimental setup. In order to maintain phase stability between the FWM signal and the reference beam, a HeNe laser propagates the same path. The HeNe light is reflected back by dichroic mirrors labeled as DCM and the interference pattern is detected with the photodiode (PD). Similarly, as implemented in the instrument (Ref. 5) any mechanical drifts are compensated using a piezoelectric transducer (PZT) driven by a high speed loop filter.

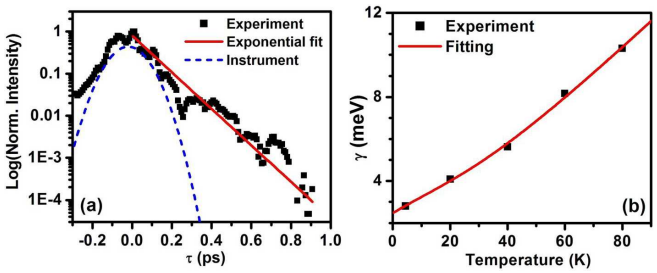

FIG. 2. (a) Time integrated FWM for T=0 fs. Black squares are the experimental data whereas the red line is a single exponential fit with $T_2 \sim 440fs$. The dashed line corresponds to the instrumental response assuming a 200 fs autocorrelation width. (b) Temperature dependence of the homogeneous width obtained from the cross diagonal profile of the 2DFT spectra. The black squares are obtained from experiment whereas the red line is fitting using Eq. (1).

linewidth. 2DFT spectra as a function of temperature were collected. The homogeneous widths obtained from the cross diagonal profile of the 2DFT spectra are plotted as a function of temperature in Fig. 2(b). The temperature dependence of the phonon broadening of excitonic transitions is thought to be caused by acoustic phonon scattering at low temperature and optical phonon scattering at higher temperature. The elastic acoustic phonon scattering leads to a linear temperature dependence and is given by the first term in Eq. (1), whereas the scattering by optical phonons is proportional to the phonon population of an average optical phonon with frequency Ω. The temperature independent term γ^* reflects the dephasing caused by the remaining contributions[19]. The fitting using Eq. (1) reproduces well the experimentally measured linewidths. Infrared absorption measurements on PbS quantum dots have shown a strong absorbtion centered around 95 cm^{-1} (11.8 meV) and attributed it to optical phonons which is chosen here as the average phonon energy Ω[20]. The fitting shown in Fig. 2 (b) leads to $a = 75.3\mu eV/K$ that indicates significant acoustic phonon scattering as compared to other nanomaterials[21].

$$\gamma = \gamma^* + aT + \frac{b}{exp(\hbar\Omega/kT - 1)} \tag{1}$$

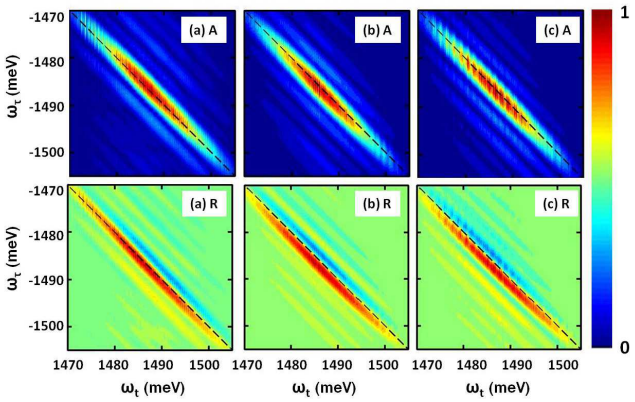

FIG. 3. Representative two-dimensional FT spectra of PbS quantum dots at 5 Kelvin for different excitation densities, (a) 1 mW, (b) 0.050 mW, and (c) 0.025 mW per excitation beam. Top the amplitudes (A) are shown, whereas bottom correspond to the real parts (R). The spectra were collected with T=0 fs. Blue (0) and red (1) correspond to the normalized intensity.

Furthermore a scattering cross section b=7.7 meV of excitons by optical phonons was also retrieved. Finally, the temperature independent dephasing leads to the offset of the curve at zero Kelvin and is γ^*=2.48 meV. Temperature dependent absorption spectra performed on the same PbS quantum dot film (not shown here) show a 12 meV reduction in broadening from room temperature to 5 Kelvin. Assuming that at 5 Kelvin the ∼160 meV width of the 1s exciton absorption peak is predominantly inhomogeneously broadened due to the size variation of the dots and performing a simple deconvolution we obtain ∼30 meV reduction in the temperature induced broadening of the homogeneous width between 5 Kelvin and room temperature. This value is in good agreement with the ∼36 meV broadening that our fitting implies if the curve is extended out to room temperature. Even if the dephasing at these temperatures is to be attributed entirely to acoustic phonon scattering, i.e., we perform a linear fit of the temperature dependence in the range between 5 and 80 K and neglect the second term in Eq. (1), a temperature independent contribution γ^* larger than 2 meV still remains.

Another common source of excitonic dephasing at low temperature in nanostructures experiencing high quantum confinement are excitation induced effects, such as exciton-exciton scattering[22]. Exciton-exciton scattering plays an important role in the dephasing of excitons in single-walled semiconducting carbon nanotubes[23]. In order to further investigate the role of excitation induced effects we performed 2DFT experiments over a broad range of excitation powers. The 2DFT spectra for three representative excitation powers are shown in Fig. 3 (a-c). Excitation powers from 1 mW and all the way to 25μW per beam were used to excite the quantum dots. However, only a negligible reduction in homogeneous linewidth was observed over the entire range. The homogeneous linewidth is measured using the cross-diagonal linewidth of the 2DFT spectra. It is difficult to accurately determine how many excitons per dot are being created from the excitation density, since it is ambiguous how many layers of dots are being excited, due in part to the fact that signal is collected in reflective geometry. However, for the lowest excitation density of 25μW at a repetition rate of $\sim$ 76 MHz and with a focal diameter of about $\sim 100\mu m$, an excitation of approximately $\sim 1 \times 10^{-3}$ excitons per quantum dot is estimated. This assessment being an upper limit since it assumes only one layer of quantum dots is excited. The long excitonic lifetime component of at least one microsecond leads to exciton accumulation in the sample within the repetition time of the laser. Taking the repetition time of the laser into account and estimating between 100-1000 excitons are being created during the course of the excitonic lifetime, the excitation density should still remain in average below one exciton per quantum dot. Since the excitonic dephasing for the lowest excitation density does not increase, we can safely exclude excitation induced effects as the cause of the remaining homogenous width. Using the method described in Ref. 24 the absolute phase of the signal was obtained and the real parts labeled with (R) in Fig. 3 were retrieved from the complex amplitudes. The projection of the real part of the 2DFT spectra on the ω_t axis was compared with differential absorption data to probe to accuracy of the retrieved phase. The dispersive line shape has been associated with many-body effects in the literature[25].

The PbS semiconductor defines a new excitonic prototype, in that both the valence band maximum and the conduction minimum originate from the L valleys of the bulk fcc Brillouin zone. Because the L valley is 8-fold degenerate including spin, the dimension of the excitonic manifold is 64. Theoretical calculations predict that the excitonic ground state is split by the intervalley coupling (IVS) into two manifolds with energy separation anywhere between 10-80 meV depending on the quantum dot diameter[11]. These manifolds are again split into spin degenerate bright (B) and dark (D) states by the electron-hole exchange interaction (ES) with an energy separation of a few meV. In the present work we focus on the dephasing mechanism of excitons in PbS quantum dots. However, transient

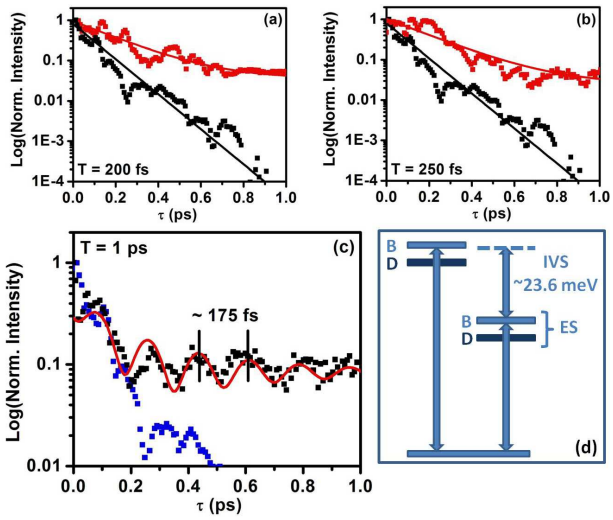

FIG. 4. Time integrated FWM for different T delays (Red) as compared to the T=0 fs FWM decay (Black) (a) T=200 fs and (b) T=250 fs. Squares represent experimental data whereas lines are the exponential fits. (c) For T=1 ps (black squares) a longer dephasing component starts to emerge and the dephasing curve exhibits periodic oscillations. The blue squares are the experimental dephasing for T=0 ps shown for comparison. The dominating rapid component observed decays at the same rate of ∼440 fs as for T=0 ps whereas the longer component has a dephasing rate of at least four picoseconds. Furthermore, the periodic quantum oscillations for T=1 ps are shown together with the fit obtained using Eq. (2) (Red line). The time integrated FWM data was collected at an excitation density of 1 mW per excitation beam. (d) Schematic of the excitonic ground state showing the two split state by the intervalley coupling (IVS) which are again split into dark (D) and bright (B) states by the electron-hole exchange (ES).

population and spin grating as well as photoluminescence lifetime measurements have provided important insights into the electronic structure of these nanostructures. Beside the known long population dynamics due to phonon-assisted single phonon thermalization and Auger nonradiative recombination, two decay components due to spin relaxation were observed, providing details into the complicated electronic structure of the excitonic ground state in PbS quantum dots[4]. The two main decay components of 290 fs and 790 fs were attributed to transitions between states arising from intervalley splitting and states split by the electron-hole exchange interaction, respectively. Furthermore, temperature dependent photoluminescence lifetime measurements on 2.5 nm diameter quantum dots have inferred a splitting of the excitonic ground state of 21.8 meV[26]. The spin relaxation studies have revealed transitions between the intervalley split states and states split by the electron-hole exchange interaction obscured in the population relaxation, which relax within the first picosecond and could possibly affect the excitonic dephasing. The time integrated FWM was measured at different T values and are shown in Fig. 4 (a-d). The time integrated FWM at T=200 fs is plotted in Fig. 4 (a) together with the data for T=0 fs for comparison. The overall decay pattern changes as compared to T=0 fs exhibiting somewhat periodic oscillations. In order to investigate the nature of these rapid oscillations T was increased by a small increment to T=250 fs, about half the period of the observed oscillations. However, no significant change in the decay was observed as indicated by the exponential fitting. At T=1 ps two distinct decay components become visible with clear periodic oscillations between them and with a period of ∼ 175 fs corresponding to an energy separation of ∼ 23.6 meV. It should be pointed out here that the dephasing rates do not change with the time delay T, but likely the intensity ratios change.

The quantum oscillations have been analyzed on the basis of a three-level model that has been used successfully in the past[27,28]. According to this model, it can be shown that the intensity of the third-order diffracted polarization is given by,

$$I(\tau) = \Theta(\tau)\left(\frac{w_1^2}{2\gamma_1} + \frac{w_2^2}{2\gamma_2} + \frac{2w_1w_2(\gamma_1+\gamma_2)}{(\gamma_1+\gamma_2)^2+(\Delta E)^2}\right) \times[w_1^2 e^{-2\gamma_1\tau} + w_2^2 e^{-2\gamma_2\tau} + 2w_1w_2 cos(\Delta E\tau)e^{-(\gamma_1+\gamma_2)\tau}] \quad (2)$$

Here Θ is the Heaviside step function, $\gamma_{1,2}$ and $w_{1,2}$ are the dephasing rates and the spectral weights of the two transitions, ΔE is the energy separation between the two levels and τ is the delay between first two pulses. The model provides a good description of the data and allows the determination of the various dephasing rates by fitting

the calculations to the experimental data. Figure 4 (c) shows a comparison of the experimental data with the calculated curve using the spectral weights $w_1 = 1$, $w_2 = 0.18$, the dephasing rates $\gamma_1^{-1} = 0.44$ ps, $\gamma_2^{-1} = 4$ ps, and $\Delta E = 23.6$ meV. The fitting model is sensitive to the dephasing rates γ_1^{-1} and γ_2^{-1}. Attempts to reproduce the quantum beats using two equally short decay components of ~ 0.44 ps lead to less adequate fitting. Small discrepancies near $\tau = 0$ ps are due to the fact that the model neglect the finite temporal width of the laser pulses. We attribute the oscillation to quantum beating between the coherently excited intervalley split excitonic states with the energy separation of 23.6 meV, whereas the longer decay component to the zero-phonon dephasing rate[18,26]. A schematic of the electronic structure of the excitonic ground state is shown in Fig. 4 (d) showing the intervalley splitting and exchange splitting into bright and dark states. Recent experimental work has demonstrated the existence of the zero-phonon dephasing in CdSe colloidal quantum dots and have attributed its dephasing time to spin flips between the dark and bright states[29]. When invoking a three-level model, there are two possibilities that could explain the origin of these quantum oscillations observed here. One of the two IVS states shown in Fig. 4 (d) could be significantly less affected by acoustic phonon scattering, allowing excitons to dephase at their zero-phonon dephasing rate or both levels are affected similarly and quantum oscillations between both dephasing components in two different levels sharing the same ground state are observed. The inhomogeneous broadening would damp the beating amplitude depending on the degree of correlation[30,31]. Coherent LO phonons can certainly generate oscillation when the time delay T is scanned which can affect the dephasing rate τ according to the oscillation period along T, but should not generate beating in τ[14]. Propagation effect can generate oscillations between two uncoupled states but are less likely in the present case since the data was collected in reflection geometry. Furthermore propagation effects lead to non-equidistant oscillations. The period of the oscillations increases as the time delay τ increases[32,33]. However, biexcitons in the presence of strong inhomogeneous broadening are shown to generate beats in the time integrated FWM signal[34–37]. In fact, the time integrated FWM technique allows one to measure precisely the biexciton binding energy in an inhomogeneously broadened system, where the inhomogeneous broadening exceeds the biexciton binding energy. In this case the period of oscillations corresponds to the biexciton binding energy. The ~ 23.6 meV separation measured in our sample would suggest a rather large binding energy. The biexciton binding energy has been measured for II-VI CdSe\ZnSe core\shell quantum dots and is in the range of ~ 20 meV[38,39]. Even larger binding energies can occur in CuCl quantum dots[40,41]. Furthermore, the biexciton binding energy can increase significantly with increasing quantum confinement[40–43]. The PbS quantum dots exhibit very strong quantum confinement due to the large exciton Bohr radius and therefore could exhibit large biexciton binding energies.

III. CONCLUSIONS

In conclusion, the dephasing mechanism of PbS colloidal quantum dots was carefully measured using time integrated FWM and 2DFT spectroscopy. The temperature dependence of the homogeneous linewidth in the temperature range of 5 to 80 K is well reproduced by a model that takes into account acoustic phonon scattering and broadening due to optical phonons. Furthermore, in addition to the dominant rapid dephasing caused by acoustic phonon scattering, a second much longer underlying component is observed. The longer component could be attributed to the zero-phonon dephasing rate. Quantum oscillations between the two components most likely originating from two different intervalley split levels are well reproduced by a simple theoretical model. Finally, it was pointed out that biexcitons can generate periodic oscillations in the time-integrated FWM decay in the presence of strong inhomogeneous broadening. The period of the oscillations would correspond to the biexciton binding energy. M.C.B and J.M.L. were supported as part of the Center for Advanced Solar Photophysics, an Energy Frontier Research Center funded by the U.S. Department of Energy, Office of Science, Office of Basic Energy Sciences. DOE funding was provided to NREL through Contract DE-AC36-086038308. *Electronic address: karaiskaj@usf.edu

[1] O. E. Semonin, J. M. Luther, S. Choi, H.-Y. Chen, J. Gao, A. J. Nozik, and M. C. Beard, Science **334**, 1530 (2011).
[2] E. H. Sargent, Nat. Photonics **6**, 133 (2012).
[3] X. Wang and G. Koleilat and J. Tang and H. Liu and I. J. Kramer and R. Debnath and L. Brzozowski and D. A. R. Barkhouse and L. Levina and S. Hoogland and E. H. Sargent, Nat. Photonics **5**, 480 (2011).
[4] J. C. Johnson, K. A. Gerth, Q. Song, J. E. Murphy, A. J. Nozik, and G. D. Scholes, Nano Lett. **8**, 1374 (2008).
[5] A. D. Bristow, D. Karaiskaj, X. Dai, T. Zhang, C. Carlsson, K. R. Hagen, R. Jimenez, and S. T. Cundiff, Review of Scientific Instruments **80**, 073108 (2009).
[6] S. T. Cundiff, Opt. Express **16**, 4639 (2008).
[7] G. Moody, M. E. Siemens, A. D. Bristow, X. Dai, D. Karaiskaj, A. S. Bracker, D. Gammon, and S. T. Cundiff, Phys. Rev. B **83**, 115324 (2011).
[8] D. Karaiskaj, A. D. Bristow, L. Yang, X. Dai, R. P. Mirin, S. Mukamel, and S. T. Cundiff, Phys. Rev. Lett. **104**, 117401 (2010).
[9] D. B. T. X. L. S. T. C. Katherine W. Stone, Kenan Gundogdu and K. A. Nelson, Science **324**, 1169 (2009).
[10] D. Turner and K. Nelson, Nature **7310**, 1089 (2010).
[11] J. M. An, A. Franceschetti, and A. Zunger, Nano Lett. **7**, 2129 (2007).
[12] J. Shah, *Ultrafast Spectroscopy of Semiconductors and Semiconductor Nanostructures* (Springer-Verlag, 1999).
[13] F. Masia, W. Langbein, I. Moreels, Z. Hens, and P. Borri, Phys. Rev. B **83**, 201309 (2011).
[14] R. W. Schoenlein, D. M. Mittleman, J. J. Shiang, A. P. Alivisatos, and C. V. Shank, Phys. Rev. Lett. **70**, 1014 (1993).
[15] D. M. Mittleman, R. W. Schoenlein, J. J. Shiang, V. L. Colvin, A. P. Alivisatos, and C. V. Shank, Phys. Rev. B **49**, 14435 (1994).
[16] T. D. Krauss and F. W. Wise, Phys. Rev. Lett. **79**, 5102 (1997).
[17] J. L. Machol, F. W. Wise, R. C. Patel, and D. B. Tanner, Phys. Rev. B **48**, 2819 (1993).
[18] P. Borri, W. Langbein, S. Schneider, U. Woggon, R. L. Sellin, D. Ouyang, and D. Bimberg, Phys. Rev. Lett. **87**, 157401 (2001).
[19] D.-S. Kim, J. Shah, J. E. Cunningham, T. C. Damen, W. Schäfer, M. Hartmann, and S. Schmitt-Rink, Phys. Rev. Lett. **68**, 1006 (1992).
[20] T. D. Krauss, F. W. Wise, and D. B. Tanner, Phys. Rev. Lett. **76**, 1376 (1996).
[21] M. W. Graham, Y.-Z. Ma, A. A. Green, M. C. Hersam, and G. R. Fleming, J. Chem. Phys. **134**, 034504 (2011).
[22] L. Schultheis, J. Kuhl, A. Honold, and C. W. Tu, Phys. Rev. Lett. **57**, 1635 (1986).
[23] K. Leo, E. O. Göbel, T. C. Damen, J. Shah, S. Schmitt-Rink, W. Schäfer, J. F. Müller, K. Köhler, and P. Ganser, Phys. Rev. B **44**, 5726 (1991).
[24] A. D. Bristow, D. Karaiskaj, X. Dai, and S. T. Cundiff, Opt. Express **16**, 18017 (2008).
[25] Tianhao Zhang and Irina Kuznetsova and Torsten Meier and Xiaoqin Li and Richard P. Mirin and Peter Thomas and Steven T. Cundiff , PNAS **104**, 14227 (2007).
[26] M. S. Gaponenko, A. A. Lutich, N. A. Tolstik, A. A. Onushchenko, A. M. Malyarevich, E. P. Petrov, and K. V. Yumashev, Phys. Rev. B **82**, 125320 (2010).
[27] K. Leo, J. Shah, E. O. Göbel, T. C. Damen, S. Schmitt-Rink, W. Schäfer, and K. Köhler, Phys. Rev. Lett. **66**, 201 (1991).
[28] K. Leo, E. O. Göbel, T. C. Damen, J. Shah, S. Schmitt-Rink, W. Schäfer, J. F. Müller, K. Köhler, and P. Ganser, Phys. Rev. B **44**, 5726 (1991).
[29] F. Masia, N. Accanto, W. Langbein, and P. Borri, Phys. Rev. Lett. **108**, 087401 (2012).
[30] P. Borri, W. Langbein, E. A. Muljarov, and R. Zimmermann, Phys. Stat. Sol. (b) **243**, 3890 (2006).
[31] S. T. Cundiff, Phys. Rev. A **49**, 3114 (1994).
[32] K. -H. Pantke and P. Schillak and B. S. Razbirin and V. G. Lyssenko and J. M. Hvam, Phys. Rev. Lett. **70**, 327 (1993).
[33] V. G. Lyssenko and J. Erland and I. Balslev and K. -H. Pantke and B. S. Razbirin and and J. M. Hvam, Phys. Rev. B **48**, 5720 (1993).
[34] E. Mayer, G. Smith, V. Heuckeroth, J. Kuhl, K. Bott, A. Schulze, T. Meier, D. Bennhardt, S. Koch, P. Thomas, R. Hey, and K. Ploog, Phys. Rev. B **50**, 14730 (1994).
[35] T. F. Albrecht, K. Bott, T. Meier, A. Schulze, M. Koch, S. T. Cundiff, J. Feldmann, W. Stolz, P. Thomas, S. W. Koch, and E. O. Göbel, Phys. Rev. B **54**, 4436 (1996).
[36] D. J. Lovering, R. T. Phillips, G. J. Denton, and G. W. Smith, Phys. Rev. Lett. **68**, 1880 (1992).
[37] H. Wang, J. Shah, T. C. Damen, and L. N. Pfeiffer, Solid State Commun. **91**, 869 (1994).
[38] V. D. Kulakovskii, G. Bacher, R. Weigand, T. Kümmell, A. Forchel, E. Borovitskaya, K. Leonardi, and D. Hommel, Phys. Rev. Lett. **82**, 1780 (1999).
[39] I. A. Akimov, J. T. Andrews, and F. Henneberger, Phys. Rev. Lett. **96**, 067401 (2006).
[40] R. Levy, L. Mager, P. Gilliot, and B. Hönerlage, Phys. Rev. B **44**, 11286 (1991).
[41] Y. Masumoto, S. Okamoto, and S. Katayanagi, Phys. Rev. B **50**, 18658 (1994).
[42] K. I. Kang, A. D. Kepner, S. V. Gaponenko, S. W. Koch, Y. Z. Hu, and N. Peyghambarian, Phys. Rev. B **48**, 15449 (1993).
[43] Y. Z. Hu, S. W. Koch, M. Lindberg, N. Peyghambarian, E. L. Pollock, and F. F. Abraham, Phys. Rev. Lett. **64**, 1805 (1990).